

Received by OSTI



Lawrence Berkeley Laboratory
UNIVERSITY OF CALIFORNIA

EARTH SCIENCES DIVISION

Presented at the 32nd U.S. Symposium on Rock Mechanics,
Norman, OK, July 10-22, 1991, and to be published
in the Proceedings

Predicting Permeability and Electrical Conductivity of Sedimentary Rocks from Microgeometry

E.M. Schlueter, R.W. Zimmerman, N.G.W. Cook, and P.A. Witherspoon

February 1991



Prepared for the U.S. Department of Energy under Contract Number DE-AC03-76SF00098

DISTRIBUTION OF THIS DOCUMENT IS UNLIMITED

DISCLAIMER

This document was prepared as an account of work sponsored by the United States Government. Neither the United States Government nor any agency thereof, nor The Regents of the University of California, nor any of their employees, makes any warranty, express or implied, or assumes any legal liability or responsibility for the accuracy, completeness, or usefulness of any information, apparatus, product, or process disclosed, or represents that its use would not infringe privately owned rights. Reference herein to any specific commercial product, process, or service by its trade name, trademark, manufacturer, or otherwise, does not necessarily constitute or imply its endorsement, recommendation, or favoring by the United States Government or any agency thereof, or The Regents of the University of California. The views and opinions of authors expressed herein do not necessarily state or reflect those of the United States Government or any agency thereof or The Regents of the University of California and shall not be used for advertising or product endorsement purposes.

Lawrence Berkley Laboratory is an equal opportunity employer.

LBL--30298

DE91 011882

Predicting Permeability and Electrical Conductivity of Sedimentary Rocks from Microgeometry

Erika M. Schlueter,^{,†} Robert W. Zimmerman,^{*}
Neville G. W. Cook,^{*,†} and Paul A. Witherspoon^{*}*

^{*}Earth Sciences Division
Lawrence Berkeley Laboratory
University of California
Berkeley, California 94720

[†]Department of Materials Science and Mineral Engineering
University of California

February 1991

This work was supported by the U.S. Department of Energy through the Assistant Secretary for Fossil Energy, Bartlesville Project Office, Advanced Extraction Process Technology (AEPT), under Contract No. DE-AC22-89BC14475 with the University of California at Berkeley, and by the Director, Office of Energy Research, Office of Basic Energy Sciences, Engineering and Geosciences Division, under Contract No. DE-AC03-76SF00098 with the Lawrence Berkeley Laboratory.

MASTER

Abstract

Hydraulic permeability and electrical conductivity of sedimentary rocks are predicted from the microscopic geometry of the pore space. The cross-sectional areas and perimeters of the individual pores are estimated from two-dimensional scanning electron micrographs of rock sections. The hydraulic and electrical conductivities of the individual pores are determined from these geometrical parameters, using Darcy's law and Ohm's law. Account is taken of the fact that the cross-sections are randomly oriented with respect to the channel axes, and for possible variation of cross-sectional area along the length of the pores. The effective medium theory from solid-state physics is then used to determine an effective average conductance of each pore. Finally, the pores are assumed to be arranged on a cubic lattice, which allows the calculation of overall macroscopic values for the permeability and the electrical conductivity. Preliminary results using Berea, Boise, Massilon and Saint-Gilles sandstones show reasonably close agreement between the predicted and measured transport properties.

INTRODUCTION

The determination of hydrologic parameters that characterize fluid flow through rock masses on a large scale (e.g., hydraulic conductivity, capillary pressure, and relative permeability) is crucial to activities such as the planning and control of enhanced oil recovery operations, and the design of nuclear waste repositories. Results of numerical simulation experiments performed to quantify the effects of the release and migration of non-condensable gas in water-saturated fractured formations highlight the impact of macroscopic transport properties such as intrinsic permeability, relative permeability, and capillary pressure (Schlueter and Pruess 1990). Indeed, a simulation is only as good as the underlying reservoir description, and therefore depends heavily on the physical properties as defined. Consequently, there is a need for a first-principle understanding of how pore morphology and other related factors can be used to predict basic hydraulic properties.

The macroscopic transport properties of porous and fractured media depend critically upon processes at the pore level, the connectivity and geometry of the pore space being most influential. The main objective of this research is to understand, through analysis and experiment, how fluids in pores affect the hydraulic and electrical properties of rocks, and to develop equations relating these macroscopic properties to the microscopic geometry and structure of the pore space. It has been our aim to assemble a comprehensive picture of a rock based on a geologically sound and physically accurate framework. The theoretical analysis has been useful in defining and ranking needed experiments, and has been able to successfully correlate measurements of important transport properties such as permeability and electrical conductivity of sandstone to the microgeometry of the pore space.

In this study, two-dimensional scanning electron microscope (SEM) micrographs of rock cross-sections have been employed to infer the hydraulic and electrical conductances of the individual pores. We assume that the pores are cylindrical tubes of

varying radius, and that they are arranged on a cubic lattice with a coordination number of 6. The hydraulic conductance of each tube is estimated from its area and perimeter, using the hydraulic radius approximation and the Hagen-Poiseuille equation, while the electrical conductance is related only to the cross-sectional area of the tube. In the section under consideration, the pore cross-sections are assumed to be randomly oriented with respect to the directions of the channel axes. The orientation effect has been corrected by means of geometrical and stereological considerations. Account is also taken of possible variation of the cross-sectional area along the length of each tube, e.g., pore necks and bulges. The effective medium theory of solid state physics is then used to replace each individual conductance with an effective average conductance. Finally, a unit cubic cell is extended to relate the effective tube conductances (hydraulic or electrical) to the continuum values of permeability and electrical conductivity. Preliminary results, using Berea, Boise, Massilon and Saint-Gilles sandstones, yield reasonable agreement between the predicted and measured transport properties, with essentially no arbitrary parameters in the model.

EFFECTIVE MEDIUM THEORY

Consider an inhomogeneous, disordered, composite system (conductive/non-conductive) in which one can define locally a given conductive property, e.g., conductance, which can be calculated from the geometry of the conductive element (e.g., the coefficient in Poiseuille's law for cylindrical tubes). This is possible as long as the dimensions of the local elements are large with respect to the scale of the conduction process involved (i.e., as long as the individual pores are wide enough so that fluid flow obeys the macroscopic Navier-Stokes equations, and is not dominated by surface effects). Such a medium can be approximated by a three-dimensional network with the same topology, in which all the conductances have a single effective value. The effective medium can be defined as one in which the macroscopic conductance is the

same as for the heterogeneous system, and therefore the effective conductance can be considered as the mean value controlling the physical property of concern. Since we are concerned with a random medium, it is assumed that no spatial correlation exists between the individual conductances. The theory leads to the requirement that when each individual conductance is replaced by the effective conductance, the flux perturbation averages out to zero. The resulting implicit equation defining the effective conductance is (Kirkpatrick 1973)

$$\left\langle \frac{C_{\text{eff}} - C_i}{(z/2 - 1)C_{\text{eff}} + C_i} \right\rangle = 0, \quad (1)$$

where the angle brackets denote an average taken with respect to the probability distribution function $p(C)$ of the individual conductances C_i , and z is the average coordination number of the network (i.e., the number of branches meeting at a node).

The effective medium theory coupled with a network of resistors has been used by Koplik et al. (1984) to predict permeability of Massilon sandstone, but the predicted value was ten times higher than the measured value. Doyen (1988) calculated transport properties of Fontainebleau sandstone that were about three times higher than the measured values. These models did not account for the fact that the two-dimensional section under consideration slices each pore at a random angle to its axis, nor for the variation of the cross-sectional area along the length of each tube, both of which are significant effects.

METHOD OF ANALYSIS

The concept of permeability allows a macroscopic description of fluid flow phenomena in porous media under a regime of sufficiently low fluid velocities (Scheidegger 1974). This property is linked to other properties of porous media, such

as capillary pressure and relative permeability. In order to understand the relationships, one has to understand how all those properties are conditioned by the connectivity and geometrical properties of the pore space. The simplest model that can be constructed is one that represents a porous medium by a bundle of straight, parallel cylindrical capillaries of uniform diameter that travel from one face of the porous medium to the other. Equations based on these type of one-dimensional model are called the Kozeny equations. The opposite extreme of this parallel case would be to assume a serial model in which all the pores are connected in series. This model is obviously as unrealistic as the the parallel model, and a realistic model lies in between the extremes.

A stereo SEM micrograph taken from pore casts of Berea sandstone is presented in Figure 1. As shown, the pore space is comprised of a three-dimensional irregular network of irregularly-shaped pores. Although an exact description of important morphological characteristics of the pore space is difficult, it is possible to isolate three main features:

1. Multiple-connectivity of the pore segments;
2. Converging-diverging cross-sections of pores;
3. Roughness and irregularity of the pore walls.

Since the actual rock geometry is too complex for any quantitative study, we have replaced it by a standard model geometry that preserves the main observed morphological features. The local conductive elements have been obtained from two-dimensional SEM micrographs of the various samples. Figure 2 shows such a micrograph of Berea sandstone. The pore space contours obtained from this serial section are shown in Figure 3. The hydraulic conductance of each tube is then estimated from its area and perimeter, using the hydraulic radius approximation in conjunction with Poiseuille's law, while only the cross-sectional area of a tube is needed in order to estimate its electrical conductance.

EFFECT OF CROSS-SECTIONAL SHAPE

According to the Hagen-Poiseuille equation, the volumetric flux of fluid through a cylindrical tube of radius r is given by

$$q = \frac{\pi r^4}{8\mu} \nabla P , \quad (2)$$

where μ is the absolute viscosity, and ∇P is the pressure gradient. We now use the hydraulic radius concept to rewrite equation 2 in a form that is applicable to non-circular pores. (As part of our analysis of the relationships between pore structure and transport properties, we have studied the effect of pore shape on permeability using the mathematical analogy between fluid flow through a cylindrical tube and elastic torsion of a cylindrical rod (Berker 1963). The results of this study show that the error involved in the hydraulic radius approximation lies well within $\pm 30\%$.) We have therefore concluded that the conductivity of a tubular pore is well approximated by the hydraulic radius theory. The hydraulic radius R_H of the tube is defined as

$$R_H = \frac{\text{area}}{\text{wetted perimeter}} = \frac{r}{2} . \quad (3)$$

Using equation 3, we can rewrite equation 2 as

$$q = \frac{R_H^2 A}{2\mu} \nabla P , \quad (4)$$

where A is the area of the tube. The hydraulic conductance of each tube is therefore (aside from a length factor, which eventually cancels out of the calculations) given by

$$C_h = \frac{R_h^2}{2} A . \quad (5)$$

Analogously, the electric conductance of each tube is

$$C_e = \frac{A}{\rho_w} , \quad (6)$$

where ρ_w is the resistivity of the fluid; this expression is exact, regardless of the pore shape.

CORRECTION FOR PORE ORIENTATION

In the two-dimensional sections under consideration, however, the pore cross-sections are randomly oriented with respect to the directions of the channel axes. The orientation effect has been corrected by means of the following geometrical and stereological considerations (cf., Underwood, 1970), which are exact for the case of circular cross-sections. For the hydraulic conductance:

$$(R_h^2 A)_{\text{actual}} = \frac{1}{2} \left\langle \frac{1}{\cos\theta(1+\cos^2\theta)} \right\rangle^{-1} (R_h^2 A)_{\text{measured}} , \quad (7)$$

where the brackets denote a spherical average for pores of random orientation, i.e.,

$$\left\langle \frac{1}{\cos\theta(1+\cos^2\theta)} \right\rangle = \frac{1}{\pi} \int_0^{\pi} \int_0^{\theta_{\max}} \frac{\sin\theta d\theta d\phi}{\cos\theta(1+\cos^2\theta)} , \quad (8)$$

with $\theta_{\max} = \arctan(L/D)$, where L/D is the maximum ratio of pore length to diameter. Using an average value of $L/D=5$, as estimated from the micrographs, we find that

$$(R_H^2 A)_{\text{actual}} = 0.32 (R_H^2 A)_{\text{measured}}. \quad (9)$$

(Evaluation of the integral appearing in equation 8 shows that the factor 0.32 in equation 9 is very insensitive to the value chosen for L/D). For the electrical conductance,

$$A_{\text{actual}} = \left\langle \frac{1}{\cos\theta} \right\rangle^{-1} A_{\text{measured}}, \quad (10)$$

where

$$\left\langle \frac{1}{\cos\theta} \right\rangle = \frac{1}{\pi} \int_0^{\pi} \int_0^{\theta_{\text{max}}} \frac{\sin\theta d\theta d\phi}{\cos\theta}. \quad (11)$$

We then have

$$A_{\text{actual}} = 0.49 A_{\text{measured}}. \quad (12)$$

CORRECTION FOR CONSTRICTIVITY

In addition, constrictions within the individual branch channels, i.e., pore necks and bulges, have been taken into account using an analysis based on a sinusoidal variation of cross-section (Figure 4). In the permeability analysis, for example, the factor accounts for the ratio of $\langle R^{-4} \rangle^{-1}$, which governs the conductance of a tube of varying radius, to $\langle R \rangle^4$, which is the value estimated from the micrographs (see Zimmerman et al. 1991 for details). We have estimated a throat-to-pore radius ratio of 0.5 from a pore cast of Berea sandstone, and tentatively use this value for each rock. Figure 4 then indicates an hydraulic constriction factor of 0.55, and an electric constriction factor of 0.86. Although some sandstones also exhibit roughness at scales much smaller

than the average pore diameter, it is known that such roughness has little effect on the hydraulic conductance (Berryman and Blair 1987), and can therefore be ignored.

Study of SEM stereo micrographs of Berea sandstone has indicated the presence of a statistically isotropic three-dimensional pore structure represented by Figure 5. These observations have led to the idealization that the pores of varying size are arranged on a cubic lattice, so that the coordination number, which is the number of pores that meet at each node, is 6. The effective medium theory from solid state physics is then used to replace each individual conductance with an effective average conductance, as follows. For a general discrete distribution of conductances, equation 1 takes the form

$$\sum_{i=1}^N \frac{C_{eff} - C_i}{(z/2-1)C_{eff} + C_i} = 0, \quad (13)$$

where the sum is over all N conductive elements. Upper and lower bounds on the effective conductivity are found from the two limiting cases $z=2$ and $z=\infty$. For $z=2$,

$$C_{eff} = \frac{N}{\sum_{i=1}^N (1/C_i)}, \quad (14)$$

whereas for $z=\infty$,

$$C_{eff} = \frac{\sum_{i=1}^N C_i}{N}. \quad (15)$$

When the coordination number is 2, the tubes are arranged in series and the effective conductance reaches its lowest possible value. On the other hand, when the

coordination number is ∞ , the tubes are arranged in parallel, and the effective conductance reaches its maximum value. Both the effective conductance and coordination number limits correspond to a one-dimensional arrangement of the tubes. For a coordination number of $z=6$, equation 13 must be solved numerically to find the effective conductance, given the individual conductances.

Finally, the individual conductors are imagined to be placed along the bonds of a cubic lattice. The continuum value of the conductances (hydraulic or electrical) can then be related to the effective conductance of the individual tubes by means of the following expression,

$$k = \frac{NC_{\text{eff}}}{\tau A_{\text{photo}}} , \quad (16)$$

where C_{eff} is the effective conductance of the individual tubes (calculated from equation 13 using $z=6$), N the number of pore elements in the micrograph, A_{photo} is the area of the photograph, and τ the tortuosity of a cubic lattice, which is exactly equal to 3 (since one-third of the pore tubes are aligned in each of the three lattice directions). Equation 16 holds for either the hydraulic or the electrical conductivity. The electrical conductivity is often quantified by the "formation factor", which is the ratio of the resistance of the brine-saturated rock to the resistance of an equal volume of brine. Comparison of equations 6 and 16 show that the formation factor can be expressed as

$$F = \frac{\tau A_{\text{photo}}}{NA_{\text{eff}}} , \quad (17)$$

where A_{eff} is the effective pore area.

RESULTS AND DISCUSSION

Preliminary results are presented in Table 1. Good agreement was found between measured and predicted permeabilities, whereas poor agreement was found for the formation factors. It should be noted that if a Kozeny-type parallel or serial model is applied instead, the permeability would be overpredicted or underpredicted by at least a factor of three.

When applying the method and evaluating our results one has to keep in mind that the effective medium theory is expected to work best when spatial fluctuations of hydraulic or current flux are small on a relative sense. Our laboratory percolation experiments in Berea sandstone, in combination with SEM analysis of the pore space, indicate that the distribution of pores and throats is more or less uniform throughout the sample. Consequently, the effective medium theory is expected to, and does, give very good results in Berea sandstone. These studies mark the beginning of our effort to understand how the important single-phase and multiphase transport parameters are related to the topology and geometry of the pore structure in reservoir rocks. At this time, it is still unclear why the permeability predictions are more accurate than the formation factor predictions. Future extensions of this work will be to predict relative (i.e., two-phase) permeabilities, and the saturation-dependence of the formation factor.

ACKNOWLEDGEMENTS

This work was supported by the U.S. Department of Energy under Contract No. DE-AC22-89BC14475, with the University of California at Berkeley, and by Contract No. DE-AC03-76SF00098, with the Lawrence Berkeley Laboratory. The authors thank Larry Myer for providing technical expertise with the experimental apparatus, Deepak Agrawal for providing Figure 2, Ron Wilson for providing assistance with the electron microscope, and Peter Persoff for providing the Boise and Saint-Gilles samples. The authors also thank Peter Persoff and Amy Davey for reviewing this paper.

REFERENCES

Berker, R. 1963. Integration des équations du mouvement d'un fluid visqueux incompressible. In *Handbuch der Physik*, Vol. 8, Pt. 2, p. 1-384. Berlin: Springer-Verlag.

Berryman, J.G. & S.C. Blair 1987. Kozeny-Carman relations and image processing methods for estimating Darcy's constant. *J. Appl. Phys.* 62(6): 2221-2228.

Chatzis, I. 1980. A network approach to analyze and model capillary and transport phenomena in porous media. Ph.D thesis, University of Waterloo, Ontario, Canada.

Doyen, P. 1988. Permeability, conductivity, and the geometry of sandstone. *J. Geophys. Res.* 93(B7): 7729-7740.

Kirkpatrick, S. 1973. Percolation and conduction. *Rev. Mod. Phys.* 45(4): 574-587.

Koplik, J., C. Lin & M. Vermette 1984. Conductivity and permeability from microgeometry. *J. Appl. Phys.* 56(11): 3127-3131.

Persoff, P., K. Pruess, S.M. Benson, Y.S. Wu, C.J. Radke, P.A. Witherspoon, & Y.A. Shikara 1989. Aqueous foams for control of gas migration and water coning in aquifer gas storage. Report LBL-27274, Lawrence Berkeley Laboratory.

Peterson, E.E. 1958. Diffusion in a pore of varying cross section. *Amer. Inst. Chem. Eng. J.* 4(3): 343-345.

Scheidegger, A.E. 1974. The physics of flow through porous media. Toronto: University of Toronto Press.

Schlueter, E. & K. Pruess 1990. Sensitivity studies on parameters affecting gas release from an underground rock cavern. Report LBL-28818, Lawrence Berkeley Laboratory.

Underwood, E.E. 1970. Quantitative stereology. Reading, Mass.: Addison-Wesley.

Zimmerman, R.W., E.M. Schlueter, N.G.W. Cook, and P.A. Witherspoon 1991. Predicting the permeability of sedimentary rocks from microgeometry. Submitted for publication.

Table 1. Permeability (in Darcy units) and formation factor (dimensionless) of four sedimentary rocks.

Rock	k(predicted)	k(measured)	F(predicted)	F(measured)
Berea	0.67	0.46	54.8	15.9
Boise	1.35	1.30 ^a	33.8	8.31 ^c
Massilon	3.10	2.50 ^b	64.9	11.8 ^b
Saint-Gilles	0.37	0.17 ^a	16.3	--

^a Persoff et al. (1989)

^b Koplik et al. (1984)

^c Chatzis (1980)



Figure 1. Stereo scanning electron micrograph of Berea sandstone. Actual width of the field is 1.14 mm. [XBB 905-4402]



Figure 2. Typical serial section of Berea sandstone. The rock is composed mainly of quartz grains (dark gray), feldspar grains (medium gray), and products of grain dissolution (light gray). The pore space is impregnated with Wood's metal alloy (white), and epoxy (black). [XBB 908-6348]

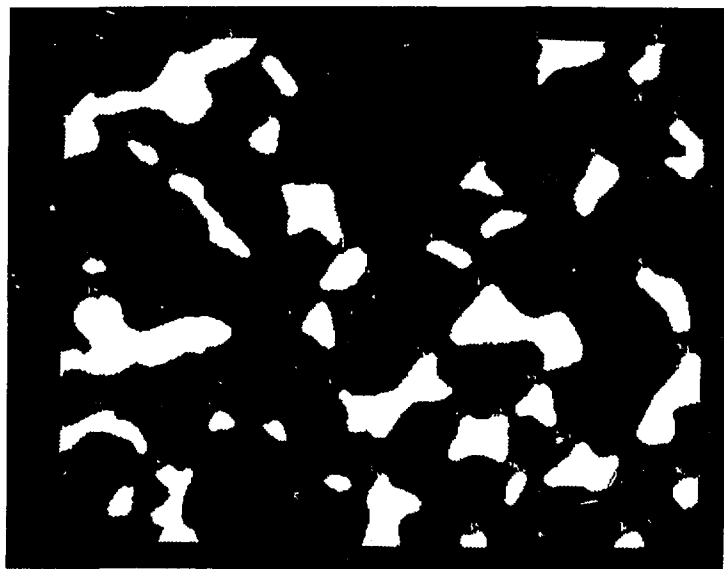


Figure 3. Pore space contours obtained from computerized image analysis of the serial section shown in Figure 2. [XBB 908-6348A]

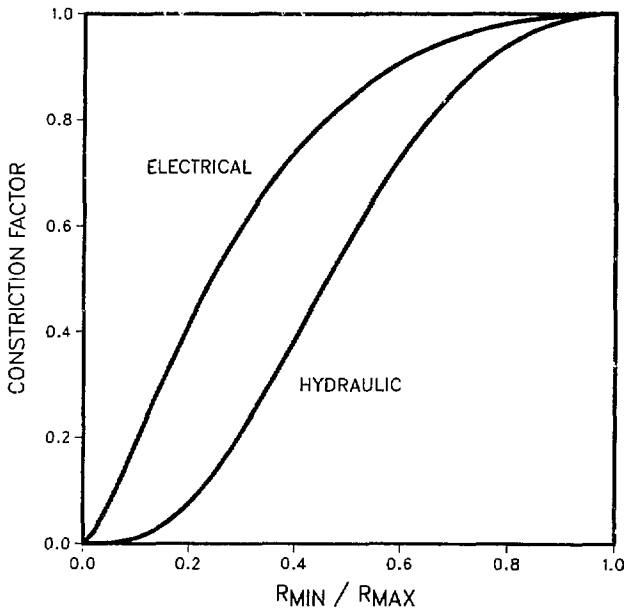


Figure 4. Constriction factors for hydraulic and electric fluxes, as functions of the ratio of the minimum pore radius to the maximum pore radius of an individual pore. The calculated conductances of the pores must be multiplied by these factors, which account for the converging-diverging nature of the pore tubes.

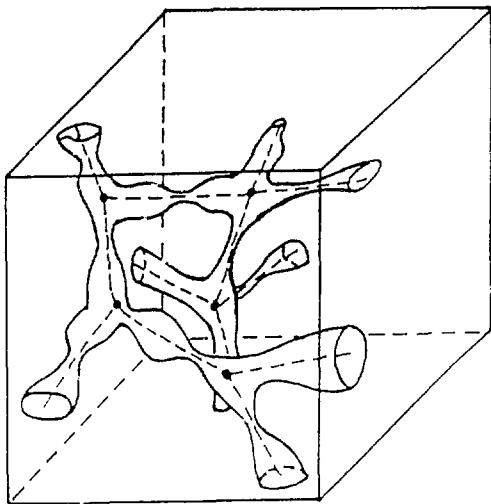


Figure 5. Schematic diagram of the "skeleton" of a microscopically inhomogeneous pore system (after Doyen 1988).